Journal of Inorganic Biochemistry 199 (2019) 110788

Contents lists available at ScienceDirect

Journal of Inorganic Biochemistry

journal homepage: www.elsevier.com/locate/jinorgbio

Preparation of polyoxometalate-doped aminosilane-modified silicate hybrid as a new barrier of chem-bio toxicant

Kuo-Hui Wu[a,*], Yin-Chiung Chang[b], Je-Chuang Wang[a]

[a] Department of Chemical and Materials Engineering, Chung Cheng Institute of Technology, National Defense University, Tahsi, Taoyuan 33551, Taiwan
[b] Department of Chemical Engineering, Army Academy, Zhongli, Taoyuan 32093, Taiwan

ARTICLE INFO

Keywords:
Polyoxometalate
Chemical toxicant
Biological toxicant
Antibacterial effect
2-Chloroethylethylsulfide

ABSTRACT

Nanohybrid membranes based on the Keggin-type polyoxometalate (POM) $H_5PV_2Mo_{10}O_{40}$ and aminosilane-modified silicate (Ormosil and Ormosil($NR_4^+Cl^-$)) hybrids were synthesized as a new barrier to protect against simulants of chemical and biological toxicant. The ^{31}P NMR and XPS results indicated that POM was bound to the Ormosil and Ormosil($NR_4^+Cl^-$) hybrids after impregnation. The antibacterial effects of the hybrids and hybrid-impregnated fabrics against Gram-negative and Gram-positive bacteria were investigated with zone of inhibition, minimum inhibitory concentration (MIC), minimum bactericidal concentration (MBC) and plate-counting method. The MIC/MBC values of Ormosil($NR_4^+Cl^-$)/POM and Ormosil/POM against bacteria were 0.267/2.67 and 2.67/26.7, respectively, and the percentage reduction of bacteria was approximately 100% after 20 laundry cycles of their fabrics. The reaction products and mechanisms of the adsorptive degradation of 2-chloroethylethylsulfide (CEES) by hybrids were investigated with ^{13}C NMR. The results of this study showed that POM-doped Ormosil systems are capable of destroying bacteria and CEES.

1. Introduction

Polyoxometalates (POMs) are an oxygen-rich class of inorganic cluster systems that exhibit remarkable chemical and physical properties, and have many promising applications in various fields, such as for catalysis, materials and medicines [1–3]. Recently, numerous reviews have discussed the design and properties of hybrid POMs in a range of systems, such as polymeric materials [4,5], surfactants [6], photocatalysts for mustard [7] and dye degradation [8], electron transport layers [9], enzyme mimics [10], and photoelectrochemical applications [11,12]. POM-based hybrid materials of current interest are summarized by Sullivan et al. in Fig. 1. [13]. POMs exert significant biological activities, with high efficacy and low toxicity. Moreover, the sizes and globular structure of many POMs are similar to some water-soluble fullerene derivatives that show excellent anti-human immunodeficiency virus (HIV) activity [14,15]. With regards to the biological activity of the POMs, many literature reports describe the activity of polyoxometalates with Keggin, lacunary Keggin, Wells-Dawson, double-Keggin and Keggin-sandwich structures against methicillin-resistant *Staphylococcus aureus* (MRSA) [16], *Helicobacter pylori* [17], SARS coronavirus (SARS-CoV) [18] and Cancer [19].

Keggin-type POM change color when they are reduced. So, if a chemical warfare agent (CWA) with an oxidizable group, such as the sulfur atom in sulfur mustard (HD), was to come into contact with the POM solution, the POM would be reduced (and the HD oxidized). As the reduced POM (POM_{Red}) and the oxidized POM (POM_{Ox}) are of different colors, the wearer would therefore have a simple indicator or warning of the presence of the CWA [20–22]. Recent reports have described the immobilization of POMs and transition metal-substituted POMs on various supports, including porous silica [23], carbon [24,25], metal–organic frameworks [26], titania [27], polymers [28,29] and organic–inorganic hybrid materials [30,31], through an organic linker, and explored their use in various organic transformations. Organically-modified silicates (Ormosils) are organic–inorganic materials formed by the hydrolysis and condensation of organically-modified silanes with traditional alkoxide precursors. In the literature survey, Ormosil materials have already been found to have many promising applications in the fields of optics, electronics, mechanics, energy, environment, biology and medicine [32–34]. Ormosils have been shown to be excellent hosts for trapping nanoparticles of metals [35,36] owing to their ability to act as stabilizers or surface-capping agents.

POM-doped aminosilane-modified silicate, Ormosil/POM and Ormosil($NR_4^+Cl^-$)/POM hybrids, have proved advantageous as a new type of insoluble antimicrobial polymer, because they have a greater antimicrobial activity and better durability in water than other conventional antimicrobial polymers. They have proved kill a broad range

* Corresponding author.
E-mail address: ccitkhwu@gmail.com (K.-H. Wu).

https://doi.org/10.1016/j.jinorgbio.2019.110788
Received 26 March 2019; Received in revised form 18 July 2019; Accepted 19 July 2019
Available online 19 July 2019

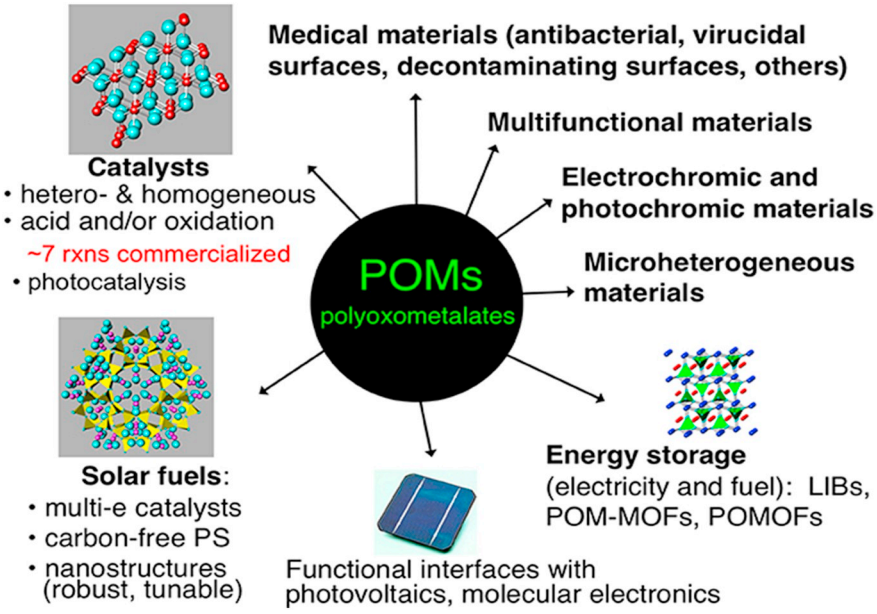

Fig. 1. Some uses and ongoing research efforts involving POMs in materials.

of microorganisms with a low minimum inhibitory concentration (MIC) and minimum bactericidal concentration (MBC) values. Ormosil is rich of chelating sites, as –OH and –NH groups, that can interact with POMs. This study described a simple method for immobilizing POMs in aminosilane-modified silicate to prepare the Ormosil/POM and Ormosil ($NR_4^+Cl^-$)/POM hybrids, and investigated the microstructures, physical properties, antibacterial activities, and ability to decompose 2-chloroethylethylsulfide (CEES). Zone of inhibition testing, MIC, MBC and the plate-counting method were used in this study to examine the antibacterial activities against Gram-negative *Pseudomonas aeruginosa* (*P. aeruginosa*), ciprofloxacin-resistant *P. aeruginosa* (CRPA), *Escherichia coli* (*E. coli*) and *E. coli* JM109, and Gram-positive *Staphylococcus aureus* (*S. aureus*), methicillin-resistant *S. aureus* (MRSA) and *Bacillus subtilis* (*B. subtilis*). Furthermore, the adsorption and oxidation reactions in the detoxification of CEES on the hybrids were studied using the NMR technique and the reaction mechanism was delineated. Moreover, the Ormosil/POM and Ormosil($NR_4^+Cl^-$)/POM hybrids with adsorption and antibacterial efficacies were incorporated into fabric matrices by impregnation to create antibacterial fabrics. Most textile materials currently used in hospitals and hotels are conducive to cross-infection or the transmission of diseases caused by microorganisms. The manufacture of dressings for medical and hygienic use has become an important area in the textile industry. These antibacterial fabrics were sterile and could be useful for wound-healing [37] and as antibacterial materials to prevent or minimize infection with pathogenic bacteria [38].

2. Experimental

2.1. Preparation of Ormosil/POM and Ormosil($NR_4^+Cl^-$)/POM hybrids

Polyoxometalate ($H_5PV_2Mo_{10}O_{40}$) was purchased from the Japanese Inorganic Chemistry Industry Joint-stock Company and was used as received. The ionic formula of water-soluble, $[PV_2Mo_{10}O_{40}]^{5-}$, and α-Keggin structure for these anions are well established [39]. POM-doped Ormosil systems were prepared as shown in Fig. 2. *N*-[3-(trimethoxysilyl)propyl]diethylenetriamine (ATS) and tetraethoxysilane (TEOS) as the precursors were used to prepare the Ormosil solution. ATS (0.04 mol) and TEOS (0.04 mol) were placed in a round-bottomed flask equipped with a stirrer and containing H_2O/C_2H_5OH, HNO_3 (0.05 M) in N_2 system, and the sol was stirred for 1 h. Another, 10 wt% POM (weight ratio 1:0.1 with respect to ATS + TEOS) was dissolved in 50 ml of an aqueous dispersion solution. The resulting solution was added to the above-described ATS/TEOS sol solution (pH = 4), and stirring was continued under N_2 at 60 °C for another 48 h. The light orange red solution was then cast onto a polytetrafluoroethylene plate and placed in a drying oven at 50 °C for 12 h, and the covalent Ormosil/POM hybrid was obtained by heat-treating the dried films at 110 °C for 2 h.

The Ormosil($NR_4^+Cl^-$)/POM hybrid was prepared as shown in Fig. 2. *N*-trimethoxysilylpropyl-*N*,*N*,*N*-trimethylammonium chloride (TMAPS), ATS and TEOS were used as the precursors to prepare the Ormosil($NR_4^+Cl^-$) solution. TMAPS (0.02 mol) and TEOS (0.04 mol) were placed in a round-bottomed flask equipped with a stirrer and containing H_2O/C_2H_5OH, HNO_3 (0.05 M) in N_2 system, and the sol was stirred for 24 h. Additional quantitative POM (weight ratio 1:0.1 with respect to TMAPS + TEOS + ATS) and ATS (0.02 mol) were dissolved in 50 mL of an aqueous dispersion solution. The resulting solution was added to the above-described TMAPS/TEOS sol solution (pH = 4), and stirring was continued under N_2 at 60 °C for another 24 h. The sol solution was then cast onto a polytetrafluoroethylene plate and placed in a drying oven at 50 °C for 12 h, and the Ormosil($NR_4^+Cl^-$)/POM hybrid was obtained by heat-treating the dried films at 110 °C for 2 h. The preparation procedure for the surface-modified fabrics was as follows: blank non-woven fabric (10 × 10 cm^2, Kang Na Hsiung Enterprise Co., Ltd.) was placed in round-bottomed flasks equipped with a stirrer, and then 30 mL of 1 mg/mL hybrid sol solution were added. The reactions were carried out for 30 min, and the resulting samples dried in a vacuum at 60 °C for 2 h.

2.2. Experimental techniques

Formation of the Ormosil/POM and Ormosil($NR_4^+Cl^-$)/POM hybrids was confirmed by UV–Vis (UV3101PC, Shimadzu, Kyoto, Japan) spectrophotometry and ^{31}P solid-state NMR systems (MSL-500, Bruker). ^{31}P NMR spectra of hybrids were obtained using the cross-polarization/magic-angle spinning (CP/MAS) technique. The morphology of the hybrids was observed using a scanning electron microscope (SEM, Hitachi S-3000N) and a transmission electron microscope (TEM, Hitachi H-7100) equipped with an energy-dispersive X-ray (EDX, Hitachi S-300) microanalysis system. X-ray photoelectron spectroscopy (XPS, PHI 1600) was applied to determine the interactions between the Ormosil systems and the POM. The hybrids were employed in a study of

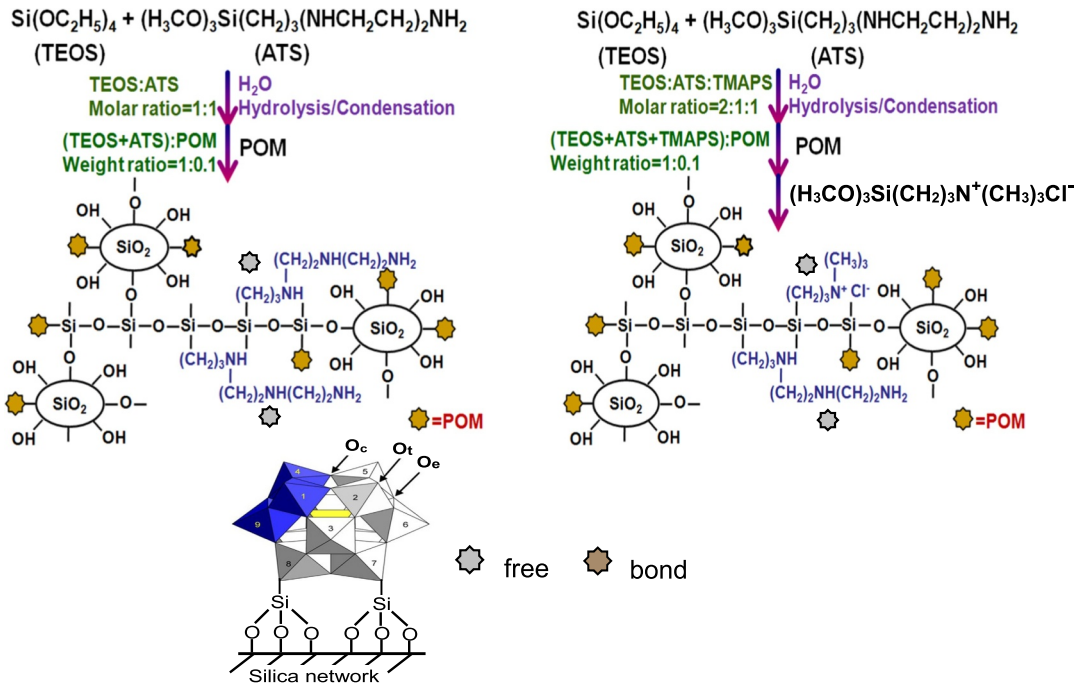

Fig. 2. Schematic illustration of the preparation of Ormosil/POM and Ormosil($NR_4^+Cl^-$)/POM hybrids.

their reaction with CEES at room temperature (27 °C). CEES was purchased from Aldrich and used as received. Reaction with CEES was examined by treating 3 mL of $CDCl_3$ solution and 10 μL of CEES with 0.2 g of the hybrid powder. After CEES loading into the hybrid powder via $CDCl_3$ had been completed, at periodic intervals of time up to 24 h, the solid reagent was immediately separated from the suspension by centrifugation. The $CDCl_3$ supernatant from centrifugation was saved for ^{13}C NMR solution analysis.

2.3. Test of antibacterial properties

P. aeruginosa, CRPA, *E. coli*, *E. coli* JM109, *S. aureus*, MRSA and *B. subtilis* were obtained from the Food Industry Research and Development Institute, Taiwan. The antibacterial spectrum of the hybrids was evaluated by zone of inhibition testing. A standard inoculum of the test organism with 10^6–10^7 colony-forming units (CFU)/mL was swabbed onto the surface of a Muller-Hinton agar plate, and discs of filter paper impregnated with antibacterial agents (6 mg/mL) were placed on the agar. The plates were incubated overnight at 37 °C, and the clear zones around the disc were measured. The antibacterial effects of the hybrids were evaluated by determination of the MIC and MBC using the broth dilution method. Tubes containing 10 mL Muller-Hinton (MH) broth with 10-fold dilutions of the samples ranging from 0.0267 to 267 mg/mL were inoculated with 4.7×10^6 CFU/mL of bacteria. The inoculated tubes were then incubated at 37 °C for 24 h, following which they were examined without shaking for visible turbidity. The MIC was determined as the lowest dilution of composite that produced no visible turbidity [40]. To determine the MBC of the hybrids, the viability of bacteria was assessed in tubes with no visible turbidity. Twenty microliters were drawn from each of the tubes and spread evenly onto an MH agar plate, followed by incubation at 37 °C for 18 h. The number of bacterial colonies was then counted [40]. The zone of inhibition, MIC and MBC methods were performed three times for each strain, and results in agreement on two or more occasions were adopted as the result of the strain.

The plate-counting method was used to further investigate the antibacterial effects of the hybrids. Approximately 10^6–10^7 CFU of *S. aureus* were cultured on MH agar plates supplemented with different concentrations of the hybrids for varying inoculation durations. A hybrid-free MH agar plate cultured under the same conditions was used as a control. The plates were incubated at 37 °C for 18 h and the numbers of colonies were counted. The test process with different concentrations was as follows: 20–100 mg of hybrids were added to 3 mL of MH broth containing 3.0×10^5 CFU/mL bacteria. The mixture was incubated aerobically at 37 °C under vibration for 24 h; 20 μL of the resulting suspension were then cultured on an MH agar plate, which was subsequently incubated at 37 °C for 18 h. The test process with different inoculation durations was as follows: 80 mg of the hybrids were added to 3 mL of MH broth containing 3.0×10^4–3.0×10^5 CFU/mL bacteria. The mixture was incubated aerobically at 37 °C under vibration for 24 h; 20 μL of the above suspension was cultured on an agar plate and incubated at 37 °C for 18 h. The bacterial concentrations were determined by measuring the optical density (OD) at 600 nm. Then, the OD values were transformed into the concentration of *S. aureus* cells.

The plate-counting method was also used to investigate the antibacterial effects of the surface-modified fabrics. Sterile water agar (0.6% agar with 0.6% NaCl in distilled water) was poured onto a sterile Petri dish to form water agar plates. Test-hybrid-coated fabrics (3 cm × 3 cm) after 0–20 laundry cycles were placed on the surfaces of the water agar plates in order to maintain moisture, and 0.2 mL of prepared 3.5×10^5 CFU/mL of *S. aureus* were spread onto the fabric samples. At each time point of 0, 4, 8, 12 and 24 h, the fabrics were transferred to a sterile test tube containing 5 mL MH broth with a few glass beads and whirled in a vortex for 2 min, followed by 10 min ultrasonic shock. Twenty microliters were drawn from each of the tubes, spread evenly onto an MH agar plate, and incubated at 37 °C for 24 h, and the number of bacterial colonies was counted. The 0–20 laundry cycles were as follows: washing of the surface-modified fabrics was according to the American Association of Textile Chemists and Colorists (AATCC) 135(1)III(A)I (alternated washing and drying). The surface-modified fabrics were washed at 40 °C under whirling (179 rpm) for 12 min and dried for 10 min. The zone of inhibition, MICs, MBCs and plate-counting methods were performed three times for each strain, and results in agreement on two or more occasions were adopted as the result of the strain. The counts of three plates corresponding to a particular sample were averaged.

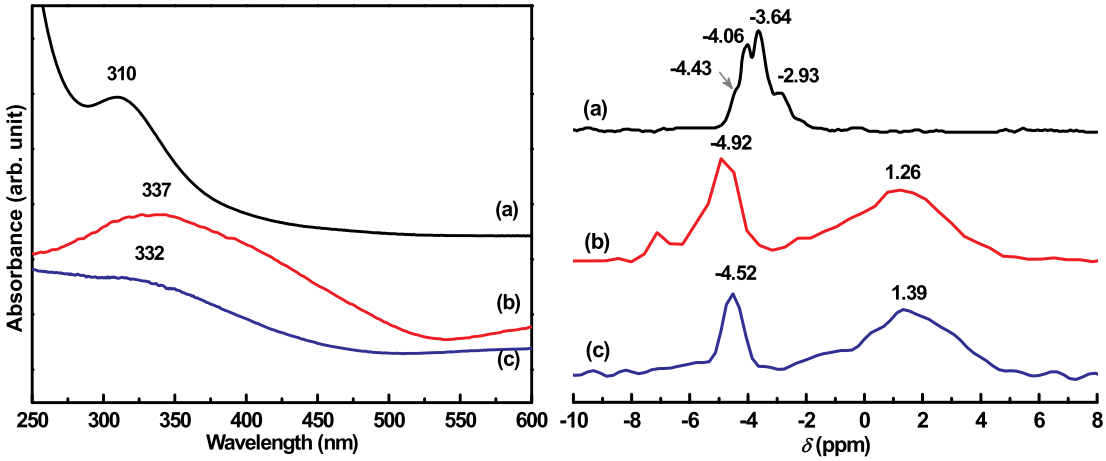

Fig. 3. UV–Vis and ^{31}P NMR spectra of the (a) POM, (b) Ormosil/POM and (c) Ormosil($NR_4^+Cl^-$)/POM hybrids.

3. Results and discussion

3.1. Structure characterization

Fig. 3 shows the UV–Vis and ^{31}P MAS-NMR spectra of the POM and hybrids: all exhibited UV absorption at approximately 310 and 332–337 nm for the POM and hybrids, respectively. The POM used in this work, $H_5PV_2Mo_{10}O_{40}$, was of a type that contains a redox-active heteroatom. These bands are generally assigned to charge transfer from the bridging oxygen to the metal in polyoxometalates [41]. The UV–Vis spectra showed broad peaks that shifted to higher wavelengths for the hybrids, which was attributed to the POM binding to the surface of the Ormosil system. ^{31}P MAS-NMR is a useful tool for detecting the local environment of the POM, as the chemical shift of the phosphorous atom depends not only on its local environment within the metal cluster, but also on factors such as associated water molecules, metal ions and solid supports. The POM solid-state MAS ^{31}P NMR exhibited two sharp and intense peaks at −3.64 and −4.06 ppm, along with shoulders at −2.93 and −4.43 ppm, typical of Keggin structures [42]. The main peak indicated the presence of P in a highly-uniform environment in a hydrated structure of POM. The small shoulders at −2.93 and −4.43 ppm were due to the presence of some P atoms in environments with differing degrees of hydration [43]. After supporting the POM on Ormosil and Ormosil($NR_4^+Cl^-$), the ^{31}P NMR signals broadened considerably, and the main peak shifted to δ = −4.92 and −4.52 ppm, respectively. Moreover, one new characteristic peak appeared at 1.26 and 1.39 ppm for Ormosil/POM and Ormosil($NR_4^+Cl^-$)/POM, respectively. These results indicated that the local environments of the P atoms in the POM had changed. The shift of the resonance signal suggested some destruction of the heteropoly anion. Thus, the broadness and new ^{31}P NMR resonances of the hybrids could be attributed to significant distortion of the heteropoly anion symmetry, and the long-range order created by water molecules in the hydrated state was lost due to a chemical interaction between the POM anion and the mesoporous Ormosil system [22].

SEM and TEM images were obtained to evaluate the surface morphology and size distribution of the POM deposited in the Ormosil system. In the SEM and EDX photographs, cured Ormosil and Ormosil ($NR_4^+Cl^-$) exhibited very dense and smooth surfaces (Fig. 4a and b). In comparison with those of the POM particles, the SEM images of the Ormosil/POM and Ormosil($NR_4^+Cl^-$)/POM hybrids were little difference. The particle size of the POM in the Ormosil($NR_4^+Cl^-$)/POM hybrid (< 20 nm) was smaller than that in the Ormosil/POM hybrid (< 50 nm), and the particles were uniformly-distributed (Fig. 4c and d). This result may be due to the action of –NH/–OH-modified Ormosil as a surface modifier that inhibited POM particle growth and prevented aggregation. TEM images of the Ormosil/POM and Ormosil($NR_4^+Cl^-$)/POM hybrids showed non-agglomerated, scattered spherical POM particles in network structure (Fig. 4e and f). EDX analysis confirmed the existence of the POM in the Ormosil matrix and qualitatively revealed the POM nanoparticle content.

In this study, we inferred that the POM chelated with the –NH/–OH groups from the Ormosil system, and a possible structure of the active POM species in the Ormosil system was proposed according to XPS. Fig. 5 shows typical XPS spectra for the POM before and after immobilization in the Ormosil system. The typical Mo_{3d} (232.9 and 236.0 eV), V_{2P} (517.1 eV) and P_{2P} (134.1 eV) XPS spectra of POM are presented. In the case of Ormosil/POM and Ormosil($NR_4^+Cl^-$)/POM, there were changes of the binding energies of Mo_{3d}, V_{2P} and P_{2P} to lower binding energies, and the Ormosil($NR_4^+Cl^-$)/POM binding energies were smaller than those of the Ormosil/POM hybrid. Moreover, the binding energy of Si_{2P} was in the order of Ormosil($NR_4^+Cl^-$)/POM > Ormosil/POM > Ormosil. These results indicated that the POM bonded with Si–OH (Si–O_t–POM) and chelated with the R–NH_2 groups (R–NH_2····POM), and the binding energy of the Si atom was enhanced, but those of Mo_{3d}, V_{2P} and P_{2P} were weakened.

3.2. Antibacterial effects

Table 1 details the zones of inhibition of the samples against bacteria. After 24 h of incubation, the zone of inhibition (13.3–16.1 mm) of the Ormosil($NR_4^+Cl^-$)/POM hybrid against bacteria was greater than that observed for Ormosil/POM (12.4–15.2 mm), and the results for Ormosil($NR_4^+Cl^-$)/POM and Ormosil/POM were greater than those observed for Ormosil (10.8–12.7 mm). The MIC and MBC values of the samples against bacteria are shown in Table 2. The MIC/MBC values of Ormosil($NR_4^+Cl^-$)/POM, Ormosil/POM and Ormosil against bacteria were 0.267/2.67, 2.67/26.7 and 26.7/ > 26.7, respectively, indicating that the antibacterial activity of the samples was of the order Ormosil ($NR_4^+Cl^-$)/POM > Ormosil/POM > Ormosil. This means that the quaternary ammoniumsilanes with trimethylammonium chloride performed better than the aminosilanes with diethylenetriamine against bacteria. POM and –$NR_4^+Cl^-$ were closely related to the antibacterial activity, which depended on the content in Ormosil. The antimicrobial mechanism of –$NR_4^+Cl^-$ has been studied extensively. Antimicrobial action in water is usually achieved on contact via the following sequence of elementary processes: adsorption onto the microbial cell surface, diffusion through the cell wall, binding and disruption of the cytoplasmic membrane, and release of cytoplasmic constituents resulting in cell death [44]. The mechanism of the antibacterial activity of POM was considered to be as follows: fluorescent X-ray analysis results showed uptake of POM into the bacterial cells. The Gram strains take

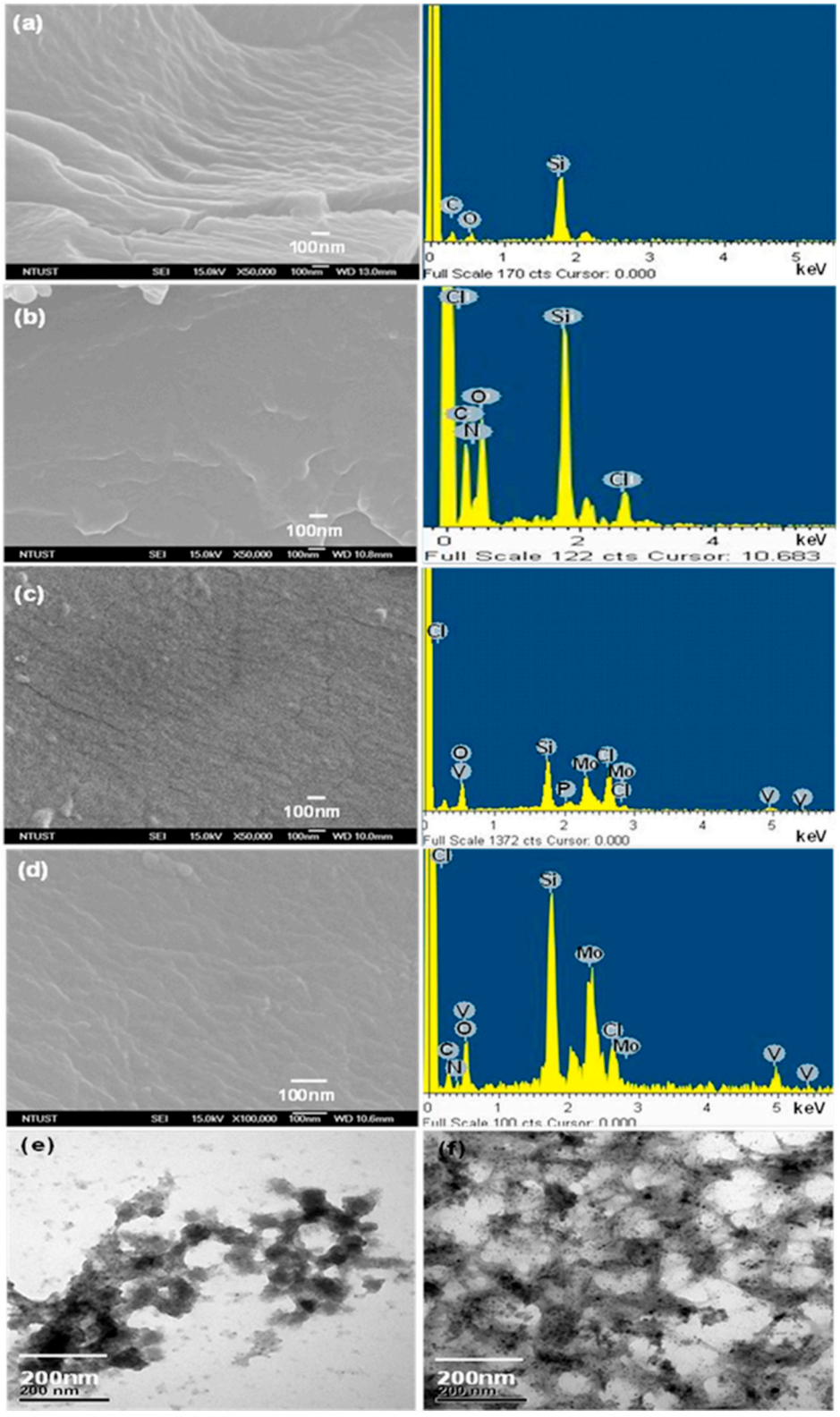

Fig. 4. SEM and EDS photographs of (a) Ormosil, (b) Ormosil($NR_4^+Cl^-$), (c) Ormosil/POM, (d) Ormosil($NR_4^+Cl^-$)/POM; TEM photographs of (e) Ormosil/POM and (f) Ormosil($NR_4^+Cl^-$)/POM.

the hydrophilic compounds into the periplasmic space through the porin protein, which is a pore-forming protein, working towards penetration of the hydrophilic compound into the outer membrane [45].

Figs. 6 and 7 show the numbers of bacterial colonies grown on MH plates as a function of the amount and inoculation duration of the Ormosil/POM and Ormosil($NR_4^+Cl^-$)/POM hybrids when approximately 4.7×10^6 CFU/mL of *S. aureus* were applied to the plates. Bacterial colonies of Gram-positive *S. aureus* were completely killed with 80 and 60 mg of Ormosil/POM and Ormosil($NR_4^+Cl^-$)/POM, respectively. Another, the dynamics of bacterial growth were also

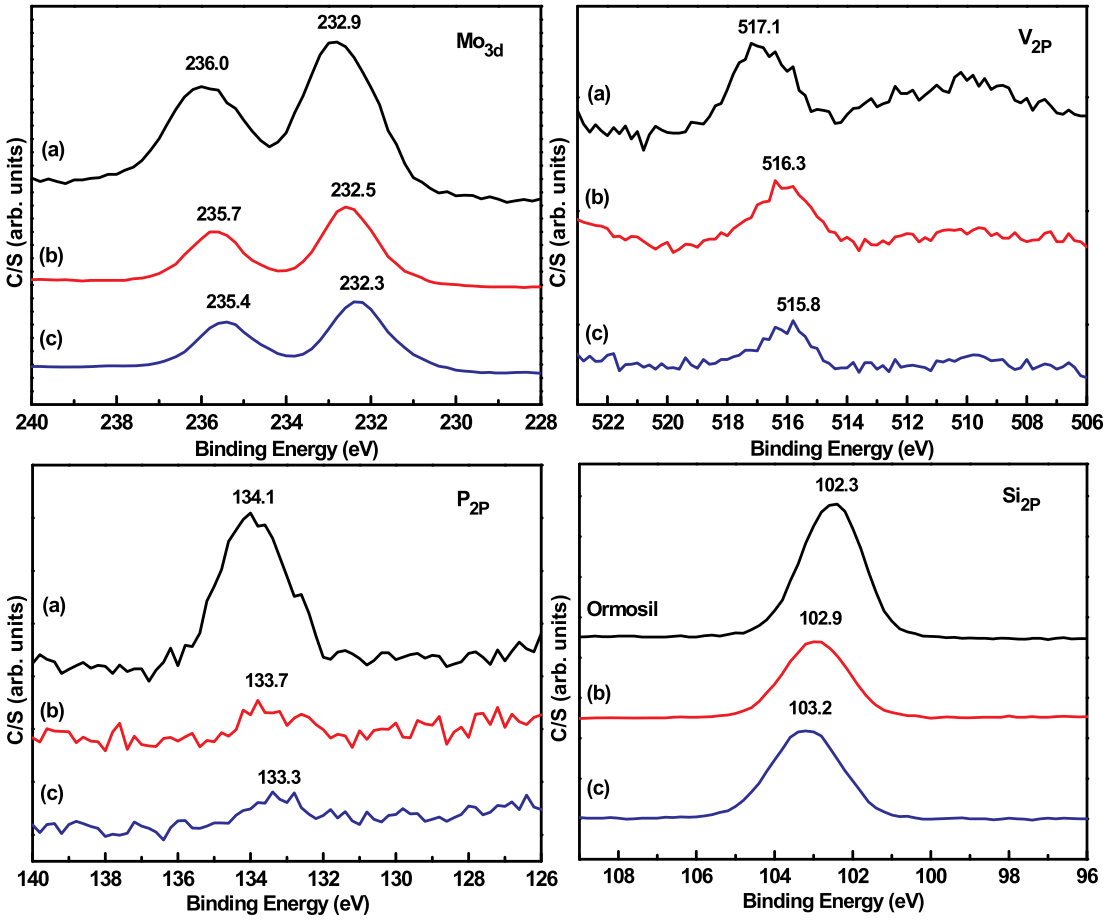

Fig. 5. XPS spectra of the (a) POM, (b) Ormosil/POM and (c) Ormosil($NR_4^+Cl^-$)/POM hybrids.

Table 1
Zone of inhibition (mm) against bacteria of the Ormosil, Ormosil/POM and Ormosil($NR_4^+C^-$)/POM hybrids.

Bacteria	Blank	Ormosil	Ormosil/POM	Ormosil($NR_4^+C^-$)/POM
S. aureus	0	11.8	14.9	15.8
B. subtilis	0	12.7	15.2	16.1
E. coli	0	11.5	13.0	13.3
P. aeruginosa	0	12.1	14.7	15.4
MRSA	0	12.7	14.5	15.3
CRPA	0	12.6	14.9	15.4
E. coli JM 109	0	10.8	12.4	13.3

Table 2
The MIC and MBC values of the Ormosil, Ormosil/POM and rmosil($NR_4^+C^-$)/POM hybrids blend on bacteria.

Bacteria	Ormosil	Ormosil/POM	Ormosil($NR_4^+C^-$)/POM
	Minimum inhibitory concentration (mg/mL)		
S. aureus	26.7	2.67	0.267
B. subtilis	26.7	2.67	0.267
E. coli	26.7	2.67	0.267
P. aeruginosa	26.7	2.67	0.267
MRSA	26.7	2.67	0.267
CRPA	26.7	2.67	0.267
E. coli JM 109	26.7	2.67	0.267
	Minimum bactericidal concentration (mg/mL)		
S. aureus	> 26.7	26.7	2.67
B. subtilis	> 26.7	26.7	2.67
E. coli	> 26.7	26.7	2.67
P. aeruginosa	> 26.7	26.7	2.67
MRSA	> 26.7	26.7	2.67
CRPA	> 26.7	26.7	2.67
E. coli JM 109	> 26.7	26.7	2.67

monitored with 4.7×10^6 CFU/mL *S. aureus* and with 80 mg/3 mL broth of hybrids under different inoculation durations. Bacterial colonies of *S. aureus* were completely killed after 36 and 24 h with Ormosil/POM and Ormosil($NR_4^+Cl^-$)/POM, respectively. Figs. 8 and 9 show the numbers of bacterial colonies grown on MH plates as a function of the number of laundry cycles of fabric-Ormosil/POM and fabric-Ormosil($NR_4^+Cl^-$)/POM when approximately 3.5×10^5 CFU/mL of *S. aureus* were applied to the plates. After 0–20 laundry cycles, the reduction in bacteria was larger than 99.9% against the *S. aureus* resistant strain after 4 h of incubation, and the percentage reduction of bacteria was approximately 100% after 24 h of incubation. From the results of Figs. 6–9, it appeared that these Ormosil/POM and Ormosil ($NR_4^+Cl^-$)/POM hybrids possessed good antibacterial action and were effective in reducing bacterial growth with 0–20 laundry cycles, possibly due to the uniform and fine distribution of POM particles on the surface of the Ormosil system. Another, the antibacterial activity of the dynamics of bacterial growth was also in the order Ormosil($NR_4^+Cl^-$)/POM > Ormosil/POM, same with the results of the MIC and MBC.

3.3. Decomposition of CEES

Fig. 10 shows the solution ^{13}C NMR spectra of the CEES compound, CEES + POM, CEES + Ormosil/POM and CEES + Ormosil($NR_4^+Cl^-$)/POM mixtures in $CDCl_3$. The results showed that CEES had δ values of 14.8 (C-1), 26.1 (C-2), 33.7 (C-3) and 43.0 ppm (C-4). For the CEES + POM mixture, CEES decomposition after 24 h led to the production of

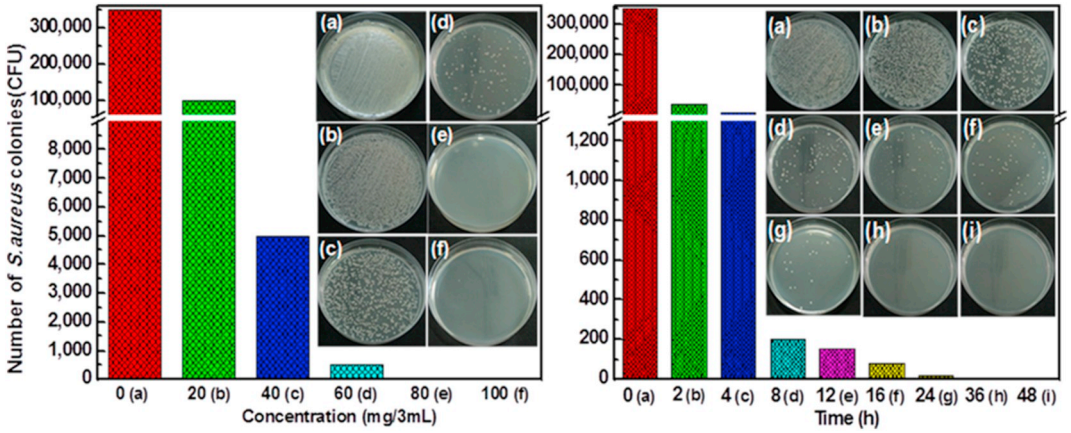

Fig. 6. Number of *S. aureus* colonies as a function of the concentration and the inoculation time (80 mg/3 mL-Broth) of Ormosil/POM composite put into 4.7×10^6 CFU of bacterial colonies. The inserted photograph of MH plates incubated under the condition in Fig. 6.

sulfoxide (CEESO), surface-bound alkoxy species (POM–$CH_2CH_2SC_2H_5$) and residual CEES. The solution ^{13}C NMR results showed that CEESO had δ values of 6.8 (C-5), 36.9 (C-6), 46.1 (C-7) and 54.2 ppm (C-8) [22], and residual CEES was also identified, with δ values at 14.8, 26.1, 33.7 and 43.0 ppm. The spectra showed peaks at 14.8 (C-1), 26.1 (C-2), 33.7 (C-3) and 29.8 ppm (C-9), which indicated that CEES was adsorbed on the POM to form a surface-bound alkoxy species. POM ($H_5PV_2Mo_{10}O_{40}$) detection of sulfides (e.g., CEES) can be explained by Eq. (1). The POM oxidizes the sulfur atom of the sulfide, yielding POM_{Red} and the oxidized form of the sulfoxide (CEESO) [21]. These results indicated the presence of oxidation and nucleophilic substitution reactions on the surface of the POM during decontamination.

$$\underset{1\ 2\ 3\ 4}{H_3C\underline{H_2}C\underline{S}C\underline{H_2}C\underline{H_2}Cl}\ (\text{CEES}) + POM_{OX} \rightarrow \underset{5\ 6\ 7\ 8}{H_3C\underline{H_2}C\underline{S}(=O)C\underline{H_2}C\underline{H_2}Cl}\ (\text{CEESO}) + POM_{Red}$$

$$\underset{1\ 2\ 3\ 4}{H_3C\underline{H_2}C\underline{S}C\underline{H_2}C\underline{H_2}Cl} + POM \rightarrow \underset{1\ 2\ 3\ 9}{H_3C\underline{H_2}C\underline{S}C\underline{H_2}C\underline{H_2}}\text{–POM} \quad (1)$$

As shown in Fig. 10c and d, the intensities of the CEES peaks were distinctly decreased, and signals of the nucleophilic substitution reaction product were seen, we guessed that the surface-bound alkoxy species (POM–$CH_2CH_2SC_2H_5$) was produced with the Ormosil/POM and Ormosil($NR_4^+Cl^-$)/POM hybrids. For the surface alkoxy complexes, we assumed that the POM offered electron-rich O_t groups and facilitated adsorption and grafting of CEES molecules via a nucleophilic substitution of the chloride. For the Ormosil/POM and Ormosil ($NR_4^+Cl^-$)/POM hybrids, no oxidation product was observed, which may be due to the low ratio of POM in the hybrids as compared with neat POM. Thus, with the Ormosil/POM and Ormosil($NR_4^+Cl^-$)/POM hybrids, CEES decomposition after 24 h led to the production of surface-bound alkoxy species (POM–$CH_2CH_2SC_2H_5$) and residual CEES.

4. Conclusions

The Ormosil/POM and Ormosil($NR_4^+Cl^-$)/POM hybrids and their impregnated fabrics possessed antibacterial abilities: their antibacterial performances against Gram-negative *P. aeruginosa*, CRPA, *E. coli* and *E. coli* JM109, and Gram-positive *S. aureus*, MRSA and *B. subtilis*, were investigated by zone of inhibition testing, MICs, MBCs and the plate-counting method, and the results showed that the hybrids exhibited low MIC/MBC values and could laundry cycles against these bacteria. The antibacterial activity of the hybrids was of the order Ormosil ($NR_4^+Cl^-$)/POM > Ormosil/POM > Ormosil. The Ormosil structure and negatively-charged anion characteristics of the POM were important in the antibacterial activity against Gram microbes. The POM was capable of reacting with CEES to form sulfoxide (CEESO) and surface-bound alkoxy species (POM–$CH_2CH_2SC_2H_5$). The Ormosil/POM and Ormosil($NR_4^+Cl^-$)/POM hybrids were capable of decomposing the adsorbed CEES to form surface-bound alkoxy species (POM–$CH_2CH_2SC_2H_5$). Thus, for the analyzed POM-doped Ormosil it was demonstrated an ability to detoxify chemical/biological toxicant by breaking down their chemical structure and destroy of bacterial growth, respectively. This type of association is novel and has great potential for use as a protective material against simulants of chemical

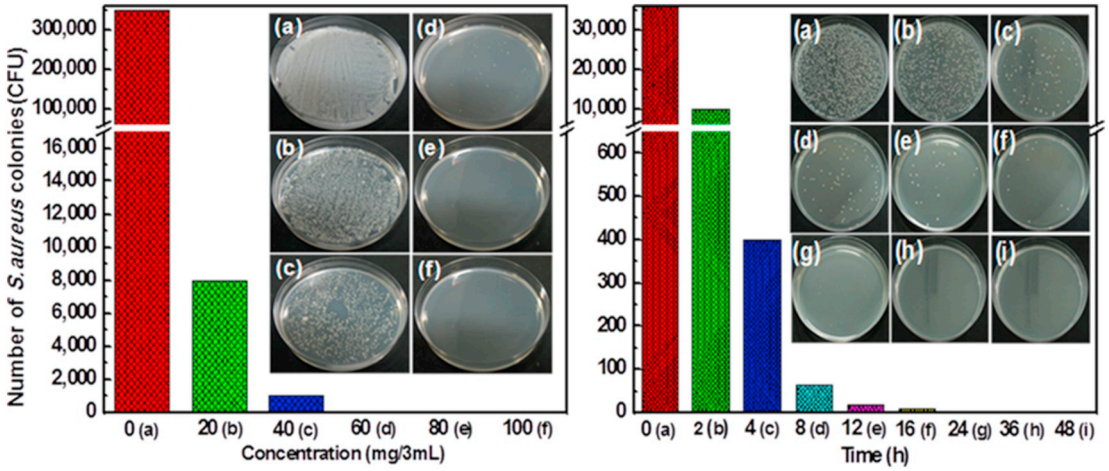

Fig. 7. Number of *S. aureus* colonies as a function of the concentration and the inoculation time (80 mg/3 mL-Broth) of Ormosil($NR_4^+Cl^-$)/POM composite put into 4.7×10^6 CFU of bacterial colonies. The inserted photograph of MH plates incubated under the condition in Fig. 7.

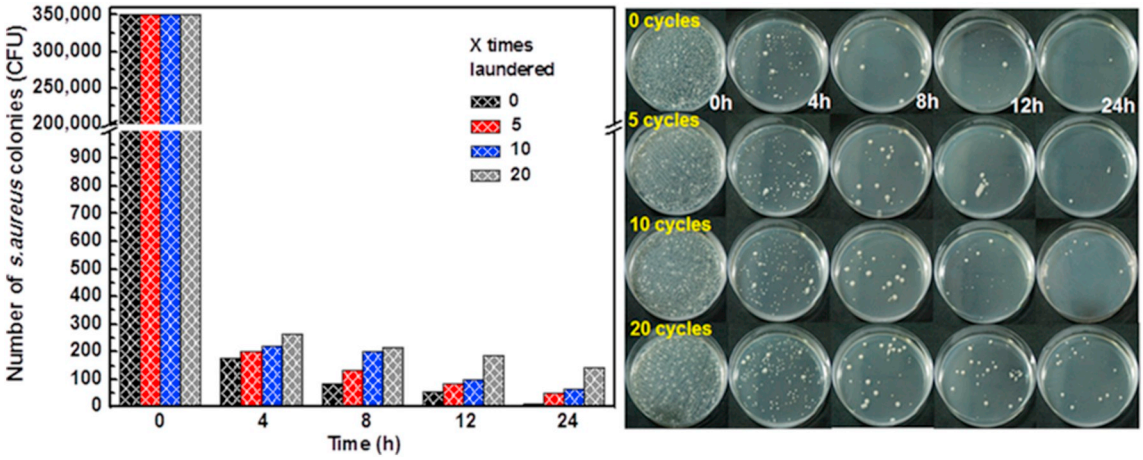

Fig. 8. Number of *S. aureus* colonies as a function of the inoculation time of Fabric-Ormosil/POM put into 3.5×10^5 CFU of bacterial colonies at after 0–20 laundering cycles. The photograph of MH plates incubated under the condition in Fig. 8.

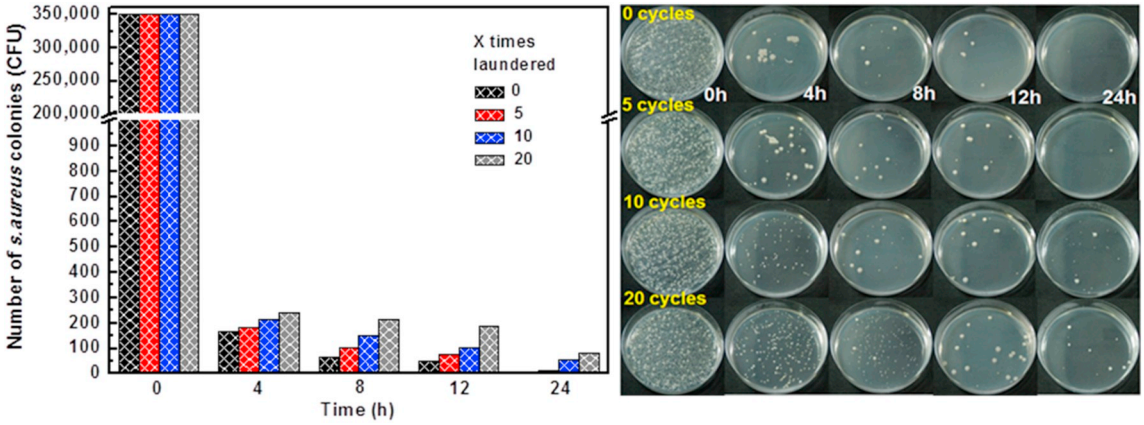

Fig. 9. Number of *S. aureus* colonies as a function of the inoculation time of Fabric-Ormosil($NR_4^+Cl^-$)/POM put into 3.5×10^5 CFU of bacterial colonies at after 0–20 laundering cycles. The photograph of MH plates incubated under the condition in Fig. 9.

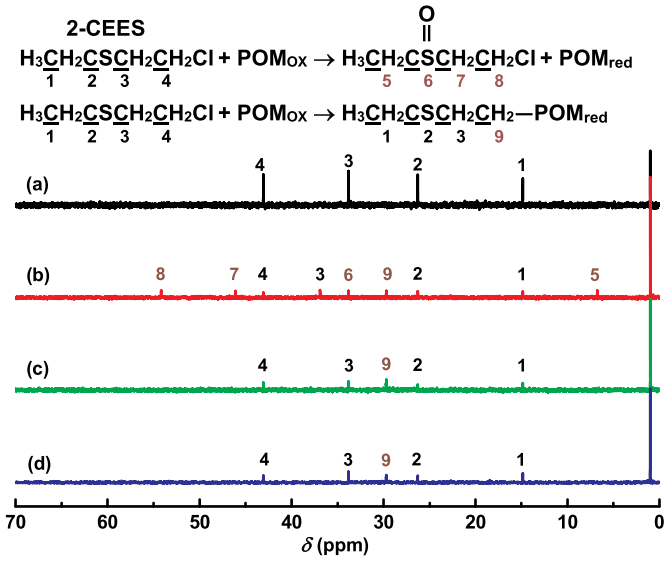

Fig. 10. Solution ^{13}C NMR spectra of (a) CEES, (b) CEES + POM, (c) CEES + Ormosil/POM and (d) CEES + Ormosil($NR_4^+Cl^-$)/POM mixtures in $CDCl_3$.

and biological toxicant. In the future, different type of Ormosil ($NR_4^+Cl^-$)/POM structures with antibacterial and detoxification of chemical toxicant will be research.

Acknowledgement

The authors thank the Ministry of Science and Technology of Taiwan for supporting this work (MOST 106-2221-E-606-014).

References

[1] Q.Y. Li, L. Zhang, J.L. Dai, H. Tang, Q. Li, H.G. Xue, H. Pang, Chem. Eng. J. 351 (2018) 441–461.
[2] L.S. Swenson, J.C. Orozco, Y. Liu, S.B. Darling, M.I. Khan, Inorg. Chem. Commun. 84 (2017) 20–23.
[3] N. Narkhede, B. Uttam, C.P. Rao, Inorg. Chimica. Acta 483 (2018) 337–342.
[4] S. Herrmann, C. Ritchie, C. Streb, Dalton Trans. 44 (2015) 7092–7104.
[5] H. Wu, H.K. Yang, W. Wang, New J. Chem. 40 (2016) 886–897.
[6] J.J. Chen, M.A. Barteau, J. Energ. Storage 13 (2017) 255–261.
[7] D.A. Giannakoudakis, J. Colón-Ortiz, J. Landers, S. Murali, M. Florent, A.V. Neimark, T.J. Bandosz, Appl. Surf. Sci. 467 (2019) 428–438.
[8] H.L. Cao, F.Y. Cai, H.B. Huang, B. Karadeniz, J. Lü, Inorg. Chem. Commun. 84 (2017) 164–167.
[9] R. Tao, Y.Z. Zhang, Z.B. Jin, Z.X. Sun, L. Xu, Electrochim. Acta 284 (2018) 10–17.
[10] R. Tian, B. Zhang, M.M. Zhao, Q. Ma, Y.F. Qi, Talanta 188 (2018) 332–338.
[11] Q. Zhang, T. Wang, Z. Sun, L. Xi, L. Xu, Sensors Actuators B Chem. 272 (2018) 289–295.
[12] X.M. Wang, L. Chen, W.L. Chen, Y.G. Li, E.B. Wang, Inorg. Chem. Commun. 96 (2018) 73–80.
[13] K.P. Sullivan, Q. Yin, D.L. Collins-Wildman, M. Tao, Y.V. Geletii, D.G. Musaev, T. Lian, C.L. Hill, Front. Chem. 6 (2018) 1–10.
[14] S.Y. Wang, W.J. Sun, Q. Hu, H. Yan, Y. Zeng, Bioorg. Med. Chem. Lett. B 27 (2017) 2357–2359.
[15] A. Flütsch, T. Schroeder, M.G. Grütter, G.R. Patzke, Bioorg. Med. Chem. Lett. 21 (2011) 1162–1166.
[16] N. Fukuda, T. Yamase, Y. Tajima, Biol. Pharm. Bull. 22 (1999) 463–470.
[17] A. Bijelic, M. Aureliano, A. Rompel, Chem. Commun. 54 (2018) 1153–1169.

[18] D.H. Hu, C. Shao, W. Guan, Z.M. Su, J.H. Sun, J. Inorg. Biochem. 101 (2007) 89–94.
[19] A. Bijelic, M. Aureliano, A. Rompel, Angew. Chem. Int. Ed. 58 (2019) 2980–2999.
[20] K.H. Wu, P.Y. Yu, C.C. Yang, G.P. Wang, C.M. Chao, Polym. Degrad. Stab. 94 (2009) 1411–1418.
[21] N.M. Okun, T.M. Anderson, C.L. Hill, J. Mol. Catal. A Chem. 197 (2003) 283–290.
[22] C.W. Kanyi, D.C. Doetschman, J.T. Schulte, Microporous Mesoporous Mater. 124 (2009) 232–235.
[23] M. Craven, D. Xiao, C. Kunstmann-Olsen, E.F. Kozhevnikova, F. Blanc, A. Steiner, I.V. Kozhevnikov, Appl. Catal., B 231 (2018) 82–91.
[24] Y. Gao, R. Gao, G. Zhang, Y. Zheng, J. Zhao, Fuel 224 (2018) 261–270.
[25] S. Chen, Y.F. Xiang, M.K. Banks, W.J. Xu, R. Wu, Appl. Surf. Sci. 466 (2019) 110–118.
[26] X.L. Wang, G. Song, H.Y. Lin, X. Wang, G.C. Liu, X. Rong, Inorg. Chem. Commun. 84 (2017) 168–173.
[27] S. Liu, X. Qu, Appl. Surf. Sci. 412 (2017) 189–195.
[28] P. Banet, C. Simonnet-Jégat, F. Goubard, S. Peralta, F. Dumur, Mater. Chem. Phys. 211 (2018) 312–320.
[29] M.L. Yola, C. Göde, N. Atar, Electrochim. Acta 246 (2017) 135–140.
[30] A.J. Kibler, G.N. Newton, Polyhedron 154 (2018) 1–20.
[31] M. Cheng, Z. Zhang, H.L. Li, G.Y. Yang, Inorg. Chem. Commun. 96 (2018) 69–72.
[32] K.H. Wu, K.F. Cheng, C.R. Wang, C.C. Yang, Y.S. Lai, Mater. Express 6 (2016) 28–36.
[33] R.N. Gillanders, I.A. Campbell, J.M.E. Glackin, I.D.W. Samuel, G.A. Turnbull, Talanta 179 (2018) 426–429.
[34] W.S. Lin, J.X. Zheng, J.N. Zhuo, H.X. Chen, X. Zhang, Surf. Coat. Technol. 345 (2018) 177–182.
[35] L.P. Gonçalves, A. Miñán, G. Benítez, M.F.L. de Mele, M.E. Vela, P.L. Schilardi, E.P. Ferreira-Neto, J.C. Noveletto, W.R. Correr, U.P. Rodrigues-Filho, Colloids Surf., B 164 (2018) 144–154.
[36] H.J. Kim, Y.G. Shul, H. Han, Appl. Catal., A 299 (2006) 46–51.
[37] L.Y. Tan, L.T. Sin, S.T. Bee, C.T. Ratnam, K.K. Woo, T.T. Tee, A.R. Rahmat, J. Vinyl Additive Technol. 25 (2019) E3–E27.
[38] N. Gokarneshan, V.B. Nagarajan, S.R. Viswanath, Biomed J Sci & Tech Res 1 (2017) 230–233.
[39] L. Petterson, I. Andersson, A. Selling, J.H. Grate, Inorg. Chem. 33 (1994) 982–993.
[40] Y. Li, P. Leung, L. Yao, J. Hosp. Infect. 62 (2006) 58–63.
[41] C.L. Hill, D.A. Bouchard, M. Kadkhodayan, M.M. Williamson, J.A. Schmidt, E.F. Hilinski, J. Am. Chem. Soc. 110 (1998) 5471–5477.
[42] C.J. Dillon, J.H. Holles, R.J. Davis, J.A. Labinger, M.E. Davis, J. Catal. 218 (2003) 54–66.
[43] S. Damyanova, L. Dimitrov, R. Mariscal, J.L.G. Fierro, L. Petrov, I. Sobrados, Appl. Catal., A 256 (2003) 183–197.
[44] J. Song, H. Kong, J. Jang, Colloids Surf., B 82 (2011) 651–656.
[45] M. Inoue, K. Segawa, S. Matsunaga, N. Matsumoto, M. Oda, T. Yamase, J. Inorg. Biochem. 99 (2005) 1023–1031.